

DETERMINING POTENTIAL ENERGY CONSTANTS FOR ATOM– AND MOLECULE–SURFACE INTERACTIONS *

Robert J. LE ROY **

Guelph-Waterloo Centre for Graduate Work in Chemistry, University of Waterloo, Waterloo, Ontario, Canada N2L 3G1

Received 18 February 1976; manuscript received in final form 4 May 1976

Methods developed for diatomic molecule spectroscopy are adapted for use in analysing the energies of atom–surface bound states in order to determine certain features of the surface-averaged potential energy function. In cases for which appropriate data are available, these simple graphical methods can yield a model-independent estimate of the potential well depth ϵ , a value for the coefficient (C_3) of the long-range z^{-3} term in the atom–surface potential, and estimates of both the total number of bound states and the energies of any unobserved levels lying near the dissociation limit. Application of these techniques to the data for atomic hydrogen on (001)LiF and NaF and for atomic helium on (001)LiF yielded: $\epsilon = 18.6(\pm 1.0)$, $18.2(\pm 3.6)$ and $8.6(\pm 0.8)$ meV, and $C_3 = 250(\pm 90)$, $180(\pm 110)$ and $95(\pm 40)$ meV Å³, respectively. Application of this approach to the data for molecular hydrogen on (001)LiF led to a new set of vibrational assignments and showed that $\epsilon = 37(\pm 4)$ meV, and that the H₂ and D₂ data of O’Keefe et al. and the H₂ binding energies which Tsuchida obtained from the data of Frisch and Stern are all internally consistent.

1. Introduction

The theory of intermolecular forces [1,2] shows that the long-range interaction potential between an atom and the planar surface of a semi-infinite solid may be expressed as a sum of inverse-power terms [3–5]:

$$V(z) = - \sum_{i \geq n} C_i / z^i, \quad (1)$$

where z is the perpendicular distance between the atom and the surface, and the asymptotically-dominant power is usually $n = 3$ ***. However, reliable experimental or theoretical methods for determining the inverse-power coefficients C_i have not

* Research supported by the National Research Council of Canada

** Alfred P. Sloan Foundation Fellow, 1974–76.

*** At very large z ($\gtrsim 100$ Å), relativistic or retardation effects change this limiting functional behaviour to z^{-4} , but the interaction energy at these distances is much too weak to influence the behaviour of the atom–surface bound states discussed here.

been reported. These constants are of particular interest because they are the features of the surface-averaged potential energy function which should be most susceptible to *ab initio* theoretical investigations. Moreover, the wide region of influence of these inverse-power terms makes them a relatively prominent part of the atom-surface interaction potential [6].

A molecule-surface bound state has translational motion parallel to the surface and quantized vibrational motion normal to it. The properties of these states have long been used as a probe of the surface-averaged potential energy function [6-17]. In these studies, the observed binding energies were usually used to define the parameters of simple model potentials, such as the Morse or Lennard-Jones (12,3) functions [13,15-17]. However, the present paper shows that analysis of such states using techniques adapted from molecular spectroscopy can yield a reliable value for the asymptotically dominant potential constant C_n , and estimates of both the total number of bound states and the energies of any unobserved levels lying near the dissociation limit. When data are available for more than one isotope, it also offers a simple procedure for clarifying the absolute vibrational numbering for the observed levels. In addition, a simple model-independent procedure for determining the depth of the surface-averaged interaction potential at its minimum is introduced.

The present methods are presented in section 2, and applied in section 3 to the data for four different systems. The discussion in section 4 then compares the present results with those obtained from previous analyses of these data, and points out certain limits on the information obtainable from atom/molecule-surface binding energies.

2. Method of analysis

The method described here is based on the fact that the distribution of levels near the dissociation limit of an anharmonic potential depends almost solely on the long-range attractive part of the potential. For potentials of the form of eq. (1), combining this fact with the first-order WKB quantization condition yields a remarkably simple expression for the binding energies, $E_b(v)$, of levels near dissociation [18,19]:

$$E_b(v) = [(v_D - v) H_n]^{2n/(n-2)}. \quad (2)$$

Here, v is the (integer) vibrational quantum number, v_D the (non-integer) semi-classical "effective" vibrational quantum number at the dissociation limit, and H_n is a constant depending only on n , the potential constant C_n , and the mass associated with the vibration, m :

$$H_n = \bar{H}_n / [m^{1/2} (C_n)^{1/n}],$$

where \bar{H}_n depends only on n . If the units of mass, length and energy are amu, Å and

meV, respectively, then $\bar{H}_n \equiv 2.02716, 3.79075, 5.43762$ and 7.02228 for $n = 3, 4, 5$ and 6 , respectively. (Note that the differences with the \bar{H}_n constants appearing in ref. [19] merely reflect a change of units and the use of more recent values [20] of the physical constants.)

For the usual molecule–surface case, $n = 3$, rearrangement of eq. (2) yields:

$$[E_b(v)]^{1/6} = 2.02716 (v_D - v)/m^{1/2} (C_3)^{1/3}. \quad (3)$$

This shows that for levels near dissociation, a plot of the one-sixth power of the binding energy versus v should be linear, with slope and intercept yielding values of C_3 and v_D . Substituting the constants thus obtained back into (3) allows this expression to be used to predict the binding energies of any as-yet unobserved levels lying near the dissociation limit. When v_D is rounded up to the next larger integer, it becomes N_{tot} , the total number of bound levels supported by the potential.

To a good approximation, the potential functions (i.e. the C_3 constants) describing the interaction potentials for different isotopic forms of a particular species, are identical. Utilizing this fact and the first order WKB quantization condition, Stwalley [21] showed that introduction of the mass-reduced vibrational quantum number

$$\eta \equiv (v + \frac{1}{2})/m^{1/2}$$

transforms eq. (2) into an expression which is exactly the same for all isotopes of the same atom. In the atom–surface problem, this implies that:

$$[E_b(\eta)]^{1/6} = 2.02716 (\eta_D - \eta)/(C_3)^{1/3}, \quad (4)$$

where $\eta_D = (v_D + \frac{1}{2})/m^{1/2}$. This is the equation used in the data analysis of section 3.

Strictly speaking, use of eqs. (2)–(4) is only valid when the longest-range term in eq. (1), C_n/z^n , makes the dominant contribution to the potential at the outer turning points of the levels in question. However, experience indicates that experimental data often obey linearized equations such as eqs. (3) and (4) for much more strongly-bound levels than this criterion would appear to allow [19,22–26]. For the inert gas Van der Waals dimers, the deviations from the $n = 6$ analogs of eqs. (3) and (4) are relatively small for even the deepest bound levels; this discrepancy is only 1.5%, 3.1% and 1.6% for the $v = 0$ levels of Ar_2 , Kr_2 and Xe_2 , respectively [24–26]. Since the surface states studied here are bound by Van der Waals type forces, use of these expressions would appear to be soundly justified.

Another potential parameter which may be determined from the plot suggested by eq. (4) is the well depth, ϵ . Since the first-order WKB eigenvalue criterion shows that a binding energy of ϵ semiclassically corresponds to $\eta = 0$ (or $v = -\frac{1}{2}$), a value of ϵ is readily obtained from a short extrapolation beyond the largest value of $E_b(\eta)$. On a plot of $E_b(\eta)$ versus η , the very sharp positive curvature would introduce large uncertainties into an extrapolation of this type. However, this curvature is greatly damped if the values of $E_b(\eta)$ are taken to a fractional power before being plotted against η . In view of its linear behaviour near dissociation, $[E_b(\eta)]^{1/6}$ would be a

particularly appropriate choice of ordinate for such plots, although other fractional powers ($1/2$, $1/3$ or $1/4$) should also suffice. An important feature of this approach is that it does not require one to assume any particular analytic form for the potential, but simply uses the fractional power to smooth the data so as to facilitate an accurate extrapolation to $\eta = 0$.

3. Applications

3.1. Atomic Hydrogen and Helium on (001) LiF and/or NaF

Reliable atom-surface bound state energies have been reported for atomic hydrogen on (001)LiF and (001)NaF [15], and for atomic He on (001) LiF [16,27]. Plots of these data in the form suggested by eq. (4) are shown in figs. 1–3; the solid lines shown there yielded the “best estimate” C_3 and η_D values presented in table 1. The quantity N_{obs} appearing in this table indicates the number of bound levels observed for each species, while N_{tot} is the total number of bound states predicted by the η_D values determined here. Also shown in these figures and table are the well depths ϵ determined from a quadratic extrapolation of $[E_b(\eta)]^{1/6}$ to $\eta = 0$.

In each of figs. 1–3, the lowest vibrational levels drop below the limiting slope associated with the levels near dissociation. Since this same behaviour occurs in the

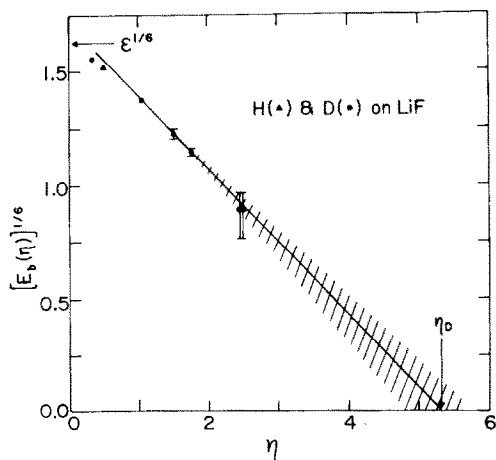


Fig. 1. For atomic hydrogen on (001)LiF, experimental binding energies [15] $E_b(\eta)$, in meV, plotted in the manner suggested by eq. (4).

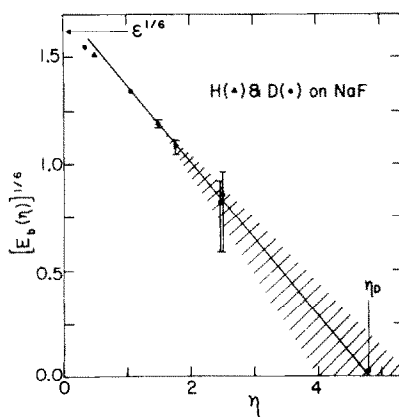


Fig. 2. For atomic hydrogen on (001)NaF, experimental binding energies [15] $E_b(\eta)$, in meV, plotted in the manner suggested by eq. (4).

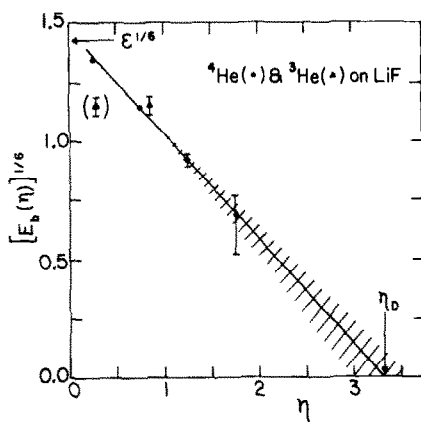


Fig. 3. For atomic helium on (001)LiF, experimental binding energies [16,27] $E_b(\eta)$, in meV, plotted in the manner suggested by eq. (4).

analogous plots for the inert gas dimers, Ar_2 , Kr_2 and Xe_2 [24–26], it appears to be a general feature of the level energies in Van der Waals interaction potentials. Consideration of the reported experimental uncertainties (error bars on points) in the light of this tendency towards negative curvature yielded the estimated near-dissociation extrapolation uncertainties indicated by the shaded regions in figs. 1–3. The error bounds on the C_3 and η_D values in table 1 correspond to lines along the upper and lower edges of these shaded regions. These figures illustrate the importance of measuring the binding energies of the highest observed levels with the utmost accuracy.

Table 1

Results obtained from figs. 1–3; N_{obs} is the number of observed levels and N_{tot} the predicted total number of bound levels for each species

System	N_{obs}	N_{tot}	η_D	C_3 (meV \AA^3)	ϵ (meV)
H on (001) LiF	3 ^a	5–6	} 5.3 (± 0.5)	250 (± 90)	18.6 (± 1.0)
D on (001) LiF	4 ^a	7–8			
H on (001) NaF	3 ^a	4–6	} 4.8 (± 0.8)	180 (± 110)	18.2 (± 3.6)
D on (001) NaF	4 ^a	6–8			
⁴ He on (001) LiF	4 ^b	6–7	} 3.3 (± 0.3)	95 (± 40)	8.6 (± 0.8)
³ He on (001) LiF	1 ^c	5–6			

^a Data from ref. [15].

^b Data from ref. [16].

^c Data from ref. [27].

Fig. 1 shows that the data for the two isotopes of atomic hydrogen bound on (001)LiF are internally consistent. Indeed, the smoothness of the resulting “combined isotopes” $E_b(\eta)$ curve (see eq. (4)) quantitatively verifies the reported [15] vibrational assignments for these data. The analogous data for H and D on (001)-NaF are not quite so well behaved; the levels for the H isotope appear to be relatively slightly more strongly bound. However, the plot in fig. 2 leaves no doubt that the reported vibrational assignments for this case are also correct. In contrast, the one bound state which O’Keefe et al. [27] observed for ^3He on (001)LiF is inconsistent with the more precise ^4He results of Meyers and Frankl [16] (round points on fig. 3) unless it is identified as $\nu = 1$ ($\eta = 0.864$; triangular point) rather than $\nu = 0$ ($\eta = 0.288$; triangular point in parentheses). Subject to this reassignment, the consistency between the data for the two He isotopes appears to confirm the absolute vibrational numbering of the observed levels.

On substituting the C_3 and η_D values obtained above back into eq. (4), predicted binding energies for as-yet unobserved levels of these systems were generated. These quantities, together with their predicted upper and lower bounds (in parentheses), are presented in table 2. Because of the anharmonicity of the potential energy curves, the dominant contributions to the probability amplitudes for such weakly bound levels would come from the neighbourhood of their outer turning point, $R_2 \simeq (C_3/E_b)^{1/3}$. For the levels considered in table 2, these turning points all lie more than 11 Å from the surface. Together with the very fine energy resolution required, this behaviour would make these predicted levels relatively difficult to observe as resonances in molecular beam scattering experiments [28].

Simple theories of the long-range induced dipole-induced dipole interaction energy [1,2] suggest that the ratio of the C_3 constants for two different species interacting with the same surface should be equal to the ratio of their polarizabilities*. It is therefore encouraging that the ratio of the present C_3 constants for atomic hydrogen and helium on (001) LiF, $250/95 = 2.6(+3.6, -1.4)$, is comparable to the ratio of the corresponding atomic polarizabilities [29], $0.6668/0.2050 = 3.3$. The approximate agreement between these ratios suggests that the uncertainties quoted in table 1 may be somewhat too large.

3.2. Molecular hydrogen on (001)LiF

O’Keefe et al. [27] have reported three molecule-surface bound state energies for each of H_2 and D_2 on (001)LiF. In contrast to the results for other systems [13,15], they reported that within the experimental uncertainties, the level energies for the two hydrogen isotopes appeared to be the same. It is now generally accepted that this conclusion is incorrect, and that it arose from the use of wrong vibra-

* Hoinkes et al. [13] correlated the polarizabilities with the well depths ϵ . However, they should really only be quantitatively compared to the attractive potential constants C_3 , since the value of ϵ also depends on the short-range repulsive forces, and the latter do not depend in a simple way on the polarizability.

Table 2
 Predicted energies and their upper and lower bounds (in parentheses), of unobserved levels of the systems considered in table 1, energies in units meV

ν	H + LiF	D + LiF	H + NaF	D + NaF	$^4\text{He} + \text{LiF}$	$^3\text{He} + \text{LiF}^a$
3	$4.3 \left(\begin{smallmatrix} 8.7 \\ 1.3 \end{smallmatrix} \right) \times 10^{-2}$	b	$12.0 \left(\begin{smallmatrix} 36.0 \\ 0.05 \end{smallmatrix} \right) \times 10^{-3}$	b	b	$3.7 \left(\begin{smallmatrix} 5.9 \\ 1.3 \end{smallmatrix} \right) \times 10^{-2}$
4	$4.1 \left(\begin{smallmatrix} 28.0 \\ 0.02 \end{smallmatrix} \right) \times 10^{-4}$	$1.1 \left(\begin{smallmatrix} 1.9 \\ 0.5 \end{smallmatrix} \right) \times 10^{-1}$	$0.3 \left(\begin{smallmatrix} 34.0 \\ c \end{smallmatrix} \right) \times 10^{-5}$	$4.2 \left(\begin{smallmatrix} 9.3 \\ 0.2 \end{smallmatrix} \right) \times 10^{-2}$	$1.1 \left(\begin{smallmatrix} 2.2 \\ 0.2 \end{smallmatrix} \right) \times 10^{-2}$	$1.1 \left(\begin{smallmatrix} 3.7 \\ 0.05 \end{smallmatrix} \right) \times 10^{-3}$
5	$c \left(\begin{smallmatrix} 4.3 \\ c \end{smallmatrix} \right) \times 10^{-7}$	$1.0 \left(\begin{smallmatrix} 2.8 \\ 0.2 \end{smallmatrix} \right) \times 10^{-2}$	c	$1.5 \left(\begin{smallmatrix} 8.8 \\ 0.0 \end{smallmatrix} \right) \times 10^{-3}$	$2.6 \left(\begin{smallmatrix} 13.0 \\ 0.02 \end{smallmatrix} \right) \times 10^{-4}$	$0.09 \left(\begin{smallmatrix} 19.0 \\ c \end{smallmatrix} \right) \times 10^{-6}$
6	c	$20.0 \left(\begin{smallmatrix} 180.0 \\ 0.02 \end{smallmatrix} \right) \times 10^{-5}$	c	$0.04 \left(\begin{smallmatrix} 16.0 \\ c \end{smallmatrix} \right) \times 10^{-5}$	$0.01 \left(\begin{smallmatrix} 49.0 \\ c \end{smallmatrix} \right) \times 10^{-7}$	c
7	c	$0.00 \left(\begin{smallmatrix} 86.0 \\ c \end{smallmatrix} \right) \times 10^{-7}$	c	$c \left(\begin{smallmatrix} 9.3 \\ c \end{smallmatrix} \right) \times 10^{-12}$	c	c

^a Interpolation on fig. 3 yields predicted binding energies of 5.4 (± 0.2), 1.7 (± 0.2) and 0.33 (± 0.1) meV for $\nu = 0, 1$ and 2, respectively.

^b Experimental value available for this level.

^c Prediction implies this level does not exist.

tional assignments for these data [30]. However, no quantitative reinterpretation of these measurements has previously been reported.

Experimental data for H_2 on (001)LiF were also reported by Frisch and Stern [7], and an analysis of their data yielded three bound state energies for this system [11]. Tsuchida later discovered errata in this analysis, and reports that the bound states seen by Frisch and Stern [7] actually have binding energies of $17.3(\pm 1.0)$, $10.0(\pm 1.0)$ and $4.3(\pm 1.0)$ meV (or 400, 230 and 100, all ± 20 cal/mole) [28]. The first two of these binding energies are in excellent agreement with those for the second and third of the levels reported by O'Keefe et al. [27], $19.1(\pm 3.8)$ and $10.0(\pm 2.0)$ meV, respectively. This agreement quantitatively confirms the reliability of both sets of measurements, and emphasizes the necessity of clarifying the vibrational assignments for this system.

Molecular hydrogen is nearly spherical [31], and the long-range attraction between H_2 or D_2 and the planar surface of a semi-infinite solid should vary as z^{-3} . Thus, the type of analysis applied (above) to atomic hydrogen and helium should also work here. Therefore, fig. 4 plots the H_2 (triangular points) and D_2 (round

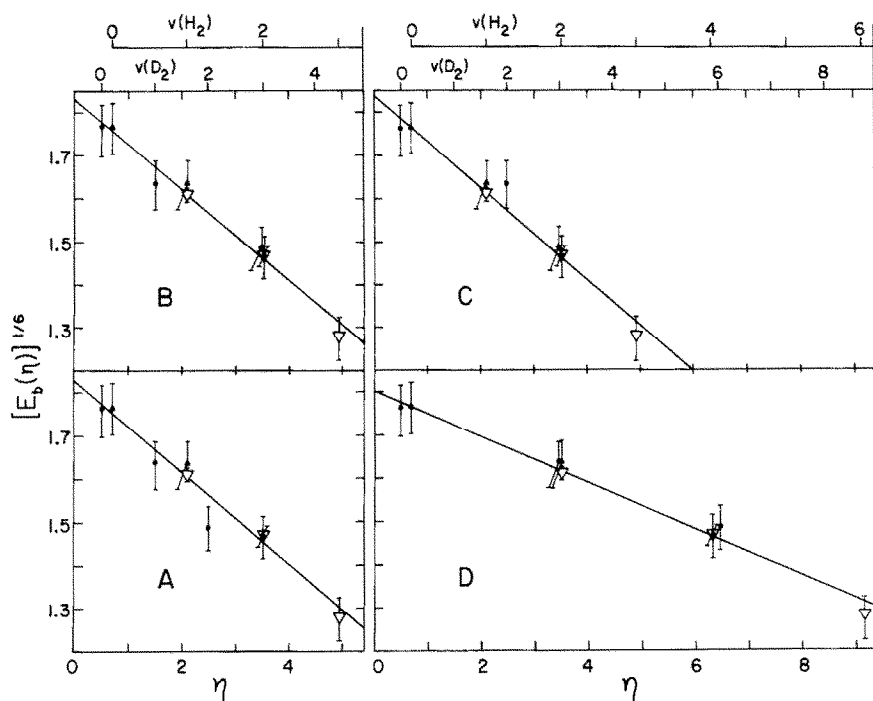


Fig. 4. For molecular hydrogen on (001)LiF, experimental binding energies of O'Keefe et al. [27] for H_2 (\blacktriangle) and D_2 (\bullet) and of Tsuchida [11,28] for H_2 (∇), in meV, plotted in the manner suggested by eq. (4), for four different sets of assumed vibrational assignments.

points) binding energies in the manner suggested by eq. (4), using four different sets of vibrational assignments. The solid points are the data of ref. [27], while the open triangles are the binding energies Tsuchida [28] obtained from the data of Frisch and Stern [7]. Case A corresponds to the original assignment of O'Keefe et al. [27], whose observed levels are identified as $\nu = 0, 1$ and 2 for both isotopes. In assignment B the highest D_2 level is assigned as $\nu = 3$; in C the two highest D_2 levels are labelled $\nu = 2$ and 3 , and in D the H_2 levels are reassigned as $\nu = 0, 2, 4$ and 6 and those for D_2 as $\nu = 0, 3$ and 6 . These appear to be the only plausible assignments for these data.

Table 3 presents the standard deviations (ERR) and the ϵ and C_3 values associated with the straight lines fitted to the points in fig. 4. The negative curvature in the small- η region of plots of this type (see figs. 1–3) means that the C_3 value determined from the slope for each case is an upper bound to the value implied by that assignment. Nevertheless, it provides an indication of the magnitude of the C_3 associated with that assignment. It is on this basis that assignment D is rejected, in spite of the linear behaviour of the data for this case. Since the polarizability of molecular hydrogen is only 1.20 times larger than that for atomic hydrogen [29,32], the C_3 value associated with assignment D is completely incompatible with the atomic hydrogen C_3 values in table 1. Moreover, while it is possible that the experiments might have missed one or two of the levels actually present, it would seem unreasonable to suggest that they overlooked eight of the fourteen levels in the given energy range. On the other hand, the differences between the data for the two isotopes make the original assignment (case A) quite unacceptable. Of the remaining possibilities, case B is preferred because of the relative magnitude of its ERR value, and because of its simplicity in requiring only one level to be reassigned. However, the additional reassignment of the second D_2 level as $\nu = 2$ (case C) cannot be completely ruled out.

In conclusion, we find that reassignment of the highest observed D_2 level [27] as $\nu = 3$ (and possibly the middle D_2 level as $\nu = 2$), together with an assignment of

Table 3

Implications of various vibrational assignments of the data [27] for H_2 and D_2 on (001)LiF

Assignment ^a	ERR (meV ^{1/6})	ϵ (meV)	C_3 (meV Å ³) ^b
A	0.026	37.3 (± 7.0)	500–1700
B ^c	0.017	37.7 (± 4.4)	630–1300
C	0.020	38.9 (± 5.5)	560–1400
D	0.015	34.3 (± 3.4)	4900–9700

^a As in fig. 4.^b Upper bound on C_3 ; see text.^c Preferred assignment.

Frisch and Stern's [7,28] H_2 levels as $v = 1, 2$ and 3 , bring the H_2 and D_2 data into good accord. The ensuing best estimate of the well depth for this case is $\epsilon = 37(\pm 4)$ meV, while rough upper bounds of $900 \text{ meV } \text{\AA}^3$ and 8.7 are obtained for C_3 and η_D , respectively. More accurate values of the latter parameters must await the observation of levels lying closer to the dissociation limit.

4. Discussion and comparisons

For potentials with inverse-power attractive tails, eq. (4) (or its analog for $n \neq 3$) will always describe the pattern of levels near dissociation. Thus, the only question associated with the use of plots such as figs. 1–4 is whether the observed levels lie sufficiently close to dissociation for this expression to apply. The small magnitude ($1/6$) of the power of $E_b(\eta)$ in eq. (4) minimizes the effect of deviations from this behaviour by the deeper levels. Hence, this procedure should be generally useful for analysing molecule–surface bound states and determining C_3 constants.

The fractional power ($1/6$) appearing in eq. (4) also allows a ready determination of reliable well depths ϵ from these plots, since it smooths the data and facilitates an accurate extrapolation to $\eta = 0$. Tsuchida has pointed out [28] that other fractional powers will serve equally well in this capacity. Using the data for H and D on LiF [15], he found that extrapolation to $\eta = 0$ on plots of $E_b(v)$ taken to the powers $1/2$, $1/3$ or $1/4$ all yielded ϵ values (18.7 , 18.8 and 18.4 meV, respectively) well within the uncertainties in the value obtained here, $18.6(\pm 1.0)$ meV. Thus, the only advantage of the $1/6$ power in this context is the fact that it allows the same plot to be used for both the near-dissociation and the potential-minimum extrapolations. On the other hand, this agreement of the ϵ values obtained using different fractional powers appears to confirm the model-independence and reliability of the present procedure for determining ϵ . Table 4 compares the present results

Table 4

Comparison of present well depths, in meV, with those obtained from previous analyses of the same data

	Present ϵ	Previous	
		Potential model	ϵ
H and D on (001)LiF	18.6 (± 1.0)	Morse ^a	17.8
H and D on (001) NaF	18.2 (± 3.6)	Morse ^a	17.9
⁴ He and ³ He on (001) LiF	8.6 (± 0.6)	Morse ^b	8.0
		zeta function ^b	8.8
		LJ (12, 3) ^b	9.3

^a From ref. [15].

^b From ref. [17].

with well depths obtained from previous “model-potential” analyses of the same data considered here.

Because its level energies are known analytic functions of the potential parameters, the Morse function is the potential form most frequently used in previous analyses of bound state energies. Wilsch and co-workers [13,15] exploited this form particularly effectively in demonstrating that the bound states for H and D on a given surface correspond to the same potential energy function, and in verifying the vibrational numbering for their data. However, since the overall distribution of the true levels is dominated by the influence of the z^{-3} potential tail, the exponential tail on the Morse function makes it unsuitable for more detailed consideration. This point is dramatically illustrated by fig. 9 in the paper by Meyers and Frankl [16], which shows how drastically the experimental vibrational spacings deviate from the linear dependence on v which is characteristic of Morse potentials.

More realistic potential forms which have been considered are the LJ (12,3) potential, and a linear combination of Riemann zeta functions [14,17], both of which have the expected long-range z^{-3} behaviour. Tsuchida used both of these functions to analyze the data for ^4He on LiF [17]. Table 5 compares his potentials to the results obtained here. In addition to the good agreement with the present C_3 and η_D values, the first four eigenvalues of his zeta function potential are in essentially exact agreement with experiment. In contrast, levels $v = 2$ and 3 of his LJ (12,3) curve are slightly too deep. Note that the total number of levels actually contained by these potentials, 7, is somewhat larger than the values $N_{\text{tot}} = 4$ and 5 reported by Tsuchida [17]. This merely reflects the fact that it is quite difficult to determine numerically the eigenvalues of levels lying very near dissociation. This problem has previously been encountered in the study of diatomic Van der Waals dimers (see “Note added in proof” in ref. [33]). It was found there that extrapolation beyond the calculated levels on plots such as figs. 1–3 often determines the number and energies of levels near dissociation more readily than does the performance of additional numerical computations.

In simple two-term potential functions, the coefficient of the long-range attractive term is usually partially dependent on the assumed functional form of the short-range repulsive wall. However, eq. (4) implies that any potential with the correct

Table 5

Comparison with previous results for He on (001)LiF obtained using potentials with z^{-3} tails

Potential	ϵ (meV)	C_3 (meV \AA^3)	η_D	N_{tot} (^4He)
LJ (12, 3) ^a	9.32	151	3.73	7
Zeta (10, 4) ^a	8.8 (± 0.3)	99 (± 15)	3.43	7
Present	8.6 (± 0.6)	95 (± 40)	3.3 (± 0.3)	6–7

^a From ref. [17].

long-range behaviour (z^{-3}) which accurately accounts for the observed distribution of levels near dissociation must have the correct C_3 . Thus, Tsuchida's procedure [17] of optimizing potential parameters by performing a least-square fit to the observed binding energies is a perfectly valid way of determining C_3 constants, as long as one obtains a good fit to the data for the highest levels. On the other hand, his method is certainly much more complicated than the present graphical procedure!

The final topic considered here is the question of the uniqueness of the potential curve obtainable from atom/molecule—surface bound state energies. The inversion of a set of vibrational energy levels to determine a potential energy curve is a problem which has been extensively studied in diatomic molecule spectroscopy. This work showed (e.g., see section 6 of ref. [19]) that the vibrational eigenvalues can be used to determine the width of the potential well as a function of its depth,

$$z_2(\eta) - z_1(\eta) = (\hbar/\sqrt{2}) \int_0^\eta [E_b(\eta') - E_b(\eta)]^{-1/2} d\eta', \quad (5)$$

where $z_1(\eta)$ and $z_2(\eta)$ are, respectively, the inner and outer turning points defined by: $V(z) = -E_b(\eta)$. However, from vibrational energies alone, there is no way of determining the individual values of $z_1(\eta)$ and $z_2(\eta)$.

In diatomic molecule spectroscopy, the rotational level spacings may be used in an expression analogous to (5) to calculate $[z_1(\eta)^{-1} - z_2(\eta)^{-1}]$, which when combined with the differences $[z_2(\eta) - z_1(\eta)]$ would yield independent values for the two turning points. However, there is no analog of this second expression in the molecule—surface problem. Thus, a knowledge of atom/molecule—surface bound state energies is *fundamentally incapable of yielding a complete potential energy curve*. The only exception to this rule applies in the region near dissociation where the fact that the distribution of energy levels depends almost solely on the long-range attractive part of the potential allows use of the procedure described in section 2. Thus, the fact that Tsuchida's zeta function potential accurately reproduces all the observed levels of ^4He on (001) LiF merely shows that his function has the correct width as a function of depth, see eq. (5), and the correct long-range tail.

The preceding discussion suggests a way of combining a knowledge of the bound-state energies with other types of experimental data in order to determine the complete atom—surface potential. Eq. (5) shows that for any assumed form of the repulsive potential in the region $z \leq z_e$, where z_e is the position of the potential minimum, the bound state data define a unique attractive potential for $z > z_e$. This constraint should greatly facilitate the accurate determination of the whole potential using fits to other types of experimental data.

Acknowledgement

I am grateful to H. Wilsch for discussions which brought this problem to my attention, to J. Doll for further stimulating my interest in it, to F.O. Goodman for a

very helpful guided tour through the relevant literature, and to J.E. Grabenstetter for his comments on the manuscript. I also gratefully acknowledge helpful correspondence with A. Tsuchida which both clarified by understanding of the new procedure for determining well depths, and brought to my attention the revised binding energies for H₂ on LiF.

References

- [1] J.O. Hirschfelder, C.F. Curtiss and R.B. Bird, *Molecular Theory of Gases and Liquids* (Wiley, New York, 1964).
- [2] J.O. Hirschfelder, Ed., *Advances in Chemical Physics*, Vol. 12, *Intermolecular Forces* (1967).
- [3] J.E. Lennard-Jones, *Trans. Faraday Soc.* 28 (1932) 333.
- [4] J. Bardeen, *Phys. Rev.* 58 (1940) 727.
- [5] H. Margenau and W.G. Pollard, *Phys. Rev.* 60 (1941) 128.
- [6] F.O. Goodman, *J. Chem. Phys.* 55 (1971) 5742.
- [7] R. Frisch and O. Stern, *Z. Physik* 84 (1933) 430.
- [8] R. Frisch, *Z. Physik* 84 (1933) 443.
- [9] J.E. Lennard-Jones and A.F. Devonshire, *Nature* 137 (1936) 1069.
- [10] A.F. Devonshire, *Proc. Roy. Soc. (London)* A156 (1936) 37.
- [11] A. Tsuchida, *Surface Sci.* 14 (1969) 375.
- [12] F.O. Goodman, *Surface Sci.* 19 (1970) 93.
- [13] H. Hoinkes, H. Nahr and H. Wilsch, *J. Phys. C (Solid State Phys.)* 5 (1972) L143.
- [14] A. Tsuchida, *Surface Sci.* 46 (1974) 611.
- [15] H-U Finzel, H. Frank, H. Hoinkes, M. Luschka, H. Nahr, H. Wilsch and U. Wonka, *Surface Sci.* 49 (1975) 557.
- [16] J.A. Meyers and D.R. Frankl, *Surface Sci.* 51 (1975) 61.
- [17] A. Tsuchida, *Surface Sci.* 52 (1975) 685.
- [18] R.J. Le Roy and R.B. Bernstein, *J. Chem. Phys.* 52 (1970) 3869.
- [19] R.J. Le Roy, in: *Molecular Spectroscopy 1, A Specialist Periodical Report of the Chemical Society of London*, Eds. R.F. Barrow, D.A. Long and D.J. Millin (1973) p. 113.
- [20] E.R. Cohen and B.N. Taylor, *J. Phys. Chem. Ref. Data* 2 (1973) 663.
- [21] W.C. Stwalley, *J. Chem. Phys.* 63 (1975) 3062.
- [22] R.F. Barrow and K.K. Yee, *J. Chem. Soc. Faraday II*, 69 (1973) 684.
- [23] R.F. Barrow, T.C. Clark, J.A. Coxon and K.K. Lee, *J. Mol. Spectrosc.* 51 (1974) 428.
- [24] R.J. Le Roy, *J. Chem. Phys.* 57 (1972) 573.
- [25] Y. Tanaka, K. Yoshino and D.E. Freeman, *J. Chem. Phys.* 59 (1973) 5160.
- [26] D.E. Freeman, K. Yoshino and Y. Tanaka, *J. Chem. Phys.* 61 (1974) 4880.
- [27] D.R. O'Keefe, J.N. Smith, Jr., R.L. Palmer and H. Saltsburg, *J. Chem. Phys.* 52 (1970) 4447.
- [28] A. Tsuchida, private communication (1976).
- [29] R.R. Teachout and R.T. Pack, *Atomic Data* 3 (1971) 195.
- [30] F.O. Goodman, private communication (1976).
- [31] W. Kolos and C.C.J. Roothan, *Rev. Mod. Phys.* 32 (1960) 219.
- [32] W. Kolos and L. Wolniewicz, *J. Chem. Phys.* 46 (1967) 1426.
- [33] K.K. Docken and T.P. Schafer, *J. Mol. Spectrosc.* 46 (1973) 454.